Published in final edited form as:
Neurobiol Dis. 2012 July ; 47(1): 102–113. doi:10.1016/j.nbd.2012.03.027.

Functional alterations in GABAergic fast-spiking interneurons in chronically injured epileptogenic neocortex

Yunyong Ma and **David A. Prince**
Dept. of Neurology and Neurological Sciences, Stanford University School of Medicine, Stanford, CA 94305 USA

Abstract

Progress toward developing effective prophylaxis and treatment of posttraumatic epilepsy depends on a detailed understanding of the basic underlying mechanisms. One important factor contributing to epileptogenesis is decreased efficacy of GABAergic inhibition. Here we tested the hypothesis that the output of neocortical fast-spiking (FS) interneurons onto postsynaptic targets would be decreased in the undercut (UC) model of chronic posttraumatic epileptogenesis. Using dual whole-cell recordings in layer IV barrel cortex, we found a marked increase in the failure rate and a very large reduction in the amplitude of unitary inhibitory postsynaptic currents (uIPSCs) from FS cells to excitatory regular spiking (RS) neurons and neighboring FS cells. Assessment of the paired pulse ratio and presumed quantal release showed that there was a significant, but relatively modest, decrease in synaptic release probability and a non-significant reduction in quantal size. A reduced density of boutons on axons of biocytin-filled UC FS cells, together with a higher coefficient of variation of uIPSC amplitude in RS cells, suggested that the number of functional synapses presynaptically formed by FS cells may be reduced. Given the marked reduction in synaptic strength, other defects in the presynaptic vesicle release machinery likely occur, as well.

Keywords

inhibition; paired recordings; barrel; fast-spiking; epilepsy

Introduction

Brain trauma can lead to delayed onset of epilepsy in man (Annegers et al., 1998; Salazar et al., 1985) and in animal models of both neocortical (Avramescu and Timofeev, 2008; D'Ambrosio et al., 2004; ECHLIN, 1959; Hoffman et al., 1994; Prince and Tseng, 1993; Ribak et al., 1982) and hippocampal injury (Buckmaster and Dudek, 1997; Lowenstein et al., 1992; McKinney et al., 1997; Tauck and Nadler, 1985). A number of alterations likely contribute to posttraumatic epileptogenesis by disturbing the delicate balance between excitation and inhibition in cortical networks. Among these pathophysiological processes, abnormalities of γ-aminobutyric acid (GABA) - mediated inhibition are prominent both in

Correspondence should be sent to: Dr. David Prince, Dept. of Neurology and Neurological Sciences, Stanford University, Room M016, Alway building, 300 Pasteur Drive, Stanford, CA 94305-5122 USA daprince@stanford.edu; Tel: 650-723-5522; Fax: 650-723-1080.

animal models (Kobayashi and Buckmaster, 2003; Luhmann et al., 1995) and resected human tissue (Loup et al., 2000; Magloczky and Freund, 2005; Williamson et al., 1999). Loss of inhibitory cells (Buckmaster and Jongen-Relo, 1999; Dinocourt et al., 2003; Marco et al., 1996) and inhibitory synapses (Kumar and Buckmaster, 2006; Marco et al., 1997; Ribak et al., 1979, 1982), changes in molecular composition of postsynaptic (Brooks-Kayal et al., 1998; Zhang et al., 2007) and extrasynaptic (Houser and Esclapez, 2003) $GABA_A$ receptors, and altered postsynaptic chloride ion (Cl^-) extrusion (Jin et al., 2005) due to effects of injury on Cl^- transport (van den Pol et al., 1996) have been reported. Less attention has been paid to the intrinsic alterations in interneuronal function and resulting effects on GABAergic neurotransmission.

The heterogeneity of interneuronal properties (Ascoli et al., 2008; Kawaguchi and Kubota, 1997; Markram et al., 2004; McBain and Fisahn, 2001), the above spectrum of pre- and postsynaptic alterations that may affect GABAergic transmission and the observations that some subgroups of interneurons are more vulnerable to injury than others (Buckmaster and Jongen-Relo, 1999; Cossart et al., 2001; Wyeth et al., 2010), make the assessment of modifications in inhibition in epileptogenic tissue a complex task requiring experiments focused on specific properties of identified classes of interneurons (Bernard et al., 2000). Our previous experiments in the partial neocortical isolation (“undercut” or UC) model of posttraumatic epileptogenesis (Graber and Prince, 2006) have shown that the frequency of miniature inhibitory postsynaptic currents (mIPSCs) and spontaneous (s)IPSCs is decreased in layer V pyramidal neurons without a significant change in mIPSC or sIPSC amplitude (Li and Prince, 2002). However, more recent results have shown abnormalities of pharmacologically isolated monosynaptic IPSCs in UC cortex, attributable to decreased release of GABA from interneuronal terminals (Faria and Prince, 2010). Information regarding the contribution of any particular subgroup of interneurons to these abnormalities, their occurrence in other lamina, or the nature of the disorder in inhibitory transmission (e.g. decreases in probability of release (Pr), numbers of inhibitory synapses (n) or quantal size (q)), is incomplete. In the present experiments, we focused on the properties of fast-spiking (FS) cells in the UC cortex because these cells form the largest interneuronal subgroup in the neocortex (Uematsu et al., 2008), and function to powerfully regulate action potential (AP) generation of excitatory cells (Maccaferri et al., 2000; Miles et al., 1996; Wang et al., 2002). Further, FS cells are known to be structurally and/or functionally abnormal in some models of epileptogenesis (Prince et al., 2009; Schwaller et al., 2004; Scotti et al., 1997; Zhang and Buckmaster, 2009).

Analysis of inhibitory transmission from these cells onto regular spiking (RS) excitatory cells and other FS cells was facilitated through use of dual whole-cell recordings of synaptically-connected pairs in UC and naïve control primary somatosensory (barrel) cortices. Results show that marked disinhibition is present in layer IV barrel cortex where output of FS cells onto RS cells and other FS cells is compromised. This loss of function is likely an outcome of several abnormalities including decreased release probability, a reduced number of functional synapses, and other potential defects in the complex machinery involved in transmitter release.

Materials and Methods

Animal preparation

All experiments were performed according to the protocols approved by the Stanford Institutional Animal Care and Use Committee. Partial cortical isolations were performed in 22 male Sprague-Dawley rats (postnatal (p) 21 days) in barrel cortex using procedures described previously (Graber and Prince, 2004). Rats were deeply anesthetized with ketamine/xylazine (80/8 mg/kg i.p.), the scalp incised, the skull exposed and a bone window

(~3 × 5 mm) opened over the barrel cortex, leaving the dura intact. A 30-gauge needle, bent to 90° ~3.5 mm from the tip, was positioned with the bent portion parallel and 3 mm lateral to the sagittal suture and the tip pointed anteriorly. The needle penetrated the dura and pia at a point 1 mm posterior to the bregma, and was advanced tangentially just beneath the pia, avoiding larger blood vessels. The bent-tip was lowered 2 mm below the cortical surface, rotated 180 degree clockwise, lifted up to just below the pia and dura, and withdrawn. A second transcortical cut, parallel and 2 mm lateral to the first, was made with the same needle. The bone window was covered with sterile plastic wrap and the scalp sutured. Injured rats were given carprofen (5 mg/kg i.p.) postoperatively and allowed to recover for 14-19 days before the terminal slice experiment.

Slice preparation and electrophysiological recording

Twenty-two UC and 20 naïve young adult (p35-40 days) male rats were used for in vitro slice recordings. Naïve and injured rats were anaesthetized with pentobarbital (55 mg/kg, i.p.) and decapitated. The brains were removed rapidly and submerged in ice-cold sucrose-based cutting solution containing (in mM): 234 sucrose, 11 D-glucose, 2.5 KCl, 1.25 NaH_2PO_4, 0.5 $CaCl_2$, 2.0 $MgSO_4$, and 26 $NaHCO_3$. Coronal slices (300 μm) were cut through barrel cortex with a vibratome (Vibratome 3000, Bannockburn, IL) and incubated, at ~35 C for ~30 min, and then at room temperature in a chamber filled with oxygenated artificial cerebrospinal fluid (ACSF) containing (in mM): 126 NaCl, 2.5 KCl, 1.25 NaH_2PO_4, 2.0 $CaCl_2$, 2.0 $MgSO_4$, 26 $NaHCO_3$, 10 D-glucose, saturated with 95% O_2/5% CO_2. Single slices were transferred to the recording chamber where they were continuously superfused at a rate of 1.5-2 ml/min with the above ACSF at 31±1 C. Patch pipettes (4–6 MΩ) were pulled from borosilicate glass capillaries (O.D./I.D., 1.5/1.1 mm, Sutter Instruments) with a Flaming-Brown micropipette puller (Model P-80/PC, Sutter Instrument, Novato, CA). Cells were directly visualized with a Zeiss Axioskop microscope (Carl Zeiss Inc., Thornwood, NY) and a 40× water immersion objective. Dual whole-cell recordings were performed within individual barrels of layer IV, using Multiclamp 700A amplifiers (Molecular Devices, Sunnyvale, CA) with 20 kHz sampling rate and a filter setting of 10 kHz. Pipettes were filled with a solution containing (in mM): 60 K-gluconate, 67 KCl, 0.1 $CaCl_2$, 10 HEPES, 1.1 EGTA, 4 ATP-Mg, and 6 phosphocreatin-tris. Biocytin (0.2%) was routinely included in the pipette solution. The pH and osmolarity of the pipette solution were adjusted to 7.2-7.3 and 275–285 mOsm, respectively with 1M KOH.

Whole-cell recordings were obtained from presynaptic FS interneurons and their target RS neurons within single layer IV barrels. The candidate FS cells were targeted based three morphological features: lack of apical dendrites, multipolar dendritic arbors, and larger soma size than that of spiny stellate cells. AP firing was evoked by 600 ms DC current injection in current clamp in both pre- and postsynaptic neurons. FS cells were distinguished from other types of inhibitory cells by their low input resistances, their narrow spike widths, fast AP firing rate during depolarization (Fig. 1C), the presence of autaptic currents (Bacci et al., 2003a), and lack of significant spike frequency adaptation measured as the ratio of the average frequency of last 5 APs to that of the first 2 APs in a ~110 Hz train of APs evoked by the above DC current pulses. RS cells were identified by their characteristic spike doublet at the onset of the depolarizing pulse (arrow in Fig. 1D) and the prominent firing frequency adaptation, as well as by their spiny dendrites seen post-hoc after histochemical processing of biocytin-filled cells. Some RS cells were also further identified in reciprocally connected pairs by showing that the unitary excitatory postsynaptic currents they evoked on FS cells were blocked by bath application of glutamate receptor antagonists. Recordings of FS and RS cells were then obtained in the voltage clamp mode. In most paired recordings, brief suprathreshold voltage steps were applied to generate escape action currents (Elfant et al., 2008; Galante and Marty, 2003; Manseau et al., 2010; Sakaba, 2008) in the presynaptic FS

cells and trigger uIPSCs in RS neurons. In 4 additional control pairs, the presynaptic FS cell was recorded in both current clamp and voltage clamp configuration so that uIPSCs evoked by action currents or action potentials could be compared. To isolate IPSCs, 20 μM 6,7-Dinitroquinoxaline-2,3-dione (DNQX) and 50 μM D-2-Amino-5-phosphonopentanoic acid (D-APV) were included in ACSF.

Estimation of quantal size

To estimate synaptic quantal size, we used two approaches: asynchronous GABA release and low calcium ACSF. In experiments using first approach, we evoked action current trains in presynaptic FS cells that were followed by asynchronous IPSCs (aIPSCs) due to presumed quantal release onto postsynaptic RS cells (Manseau et al., 2010). Three hundred – 450 ms (355 ± 11 ms, n = 10) trains of escape action currents with a firing frequency of 236 ± 11 Hz (range 160-270 Hz) were elicited in voltage-clamped FS cells at intervals of 30 sec. To minimize contamination arising from spontaneous IPSCs during the asynchronous release period and promote a high ratio of asynchronous to spontaneous release, 4 mM Sr^{2+} was substituted for 2 mM Ca^{2+} and Mg^{2+} was increased to 4 mM in the ACSF. To obtain measurements of individual events, we first recorded the frequency and amplitude of sIPSCs that occurred over 1 sec prior to the stimulus train. We then measured the same parameters for events that occurred within a 300 ms time window following the stimulus train, after initial summated postsynaptic responses returned to baseline. The mixed IPSCs during this period consisted of aIPSCs and sIPSCs. Ten-15 (14.4±0.5) sweeps per pair were quantified in 10 pairs. To evaluate the contribution that sIPSCs made to the mixed IPSCs, a correction factor (cf) was applied and defined as the percentage of the average number of sIPSCs per 300 msec prior to the stimulus train to the number of mixed IPSCs per 300 msec following the train. Only paired recordings with cf < 33.3% were analyzed. To obtain mean amplitude of aIPSCs, contamination by sIPSCs was subtracted from mixed IPSCs according to the following equation: $\frac{Amp\_mixed - Amp\_s \times cf}{1-cf}$, where Amp_s and Amp_mixed represent the average IPSC amplitude during the 1-sec and 300-ms measurement time window, respectively. The second approach we used to estimate quantal size involved perfusion of slices with ACSF containing 0.5 mM Ca^{2+} / 3.5 mM Mg^{2+}. When this perfusate increased synaptic failure rate to >80%, presumed quantal events were recorded.

Biocytin immunofluorescence staining and quantification of bouton density

To verify cell type anatomically, slices (300 μm thickness) containing biocytin-filled cells were fixed in 4% paraformaldehyde in 0.1M PB at 4°C overnight. After rinsing with PBS, slices were incubated in 10% normal goat serum with 2% BSA and 0.5% Triton X-100 in PBS and then exposed to Texas Red Avidin D (Vector Laboratory, Burlingame CA). Anatomically, RS cells were distinguished from FS cells by their spiny dendrites. Further, the slices containing well-filled FS cells were incubated for 48 hours with the primary antibody for vesicular GABA transporter (VGAT) (a generous gift from Dr. Richard Reimer, at a dilution of 1:500) to verify that swellings along interneuronal axons were GABAergic boutons (results not shown). Three terminal axonal segments were randomly selected from each of 4 control and 4 UC well-filled FS cells. Confocal image stacks of biocytin-filled FS interneurons were obtained from 150 μm thick fixed coverslipped sections with a 0.2 μm optical distance at 63× using a zoom factor of 2. This allowed tracing of randomly-selected well-filled axons from somata to their terminal arbors. A pinhole of 1 air unit and identical setting values for detector gain and amplifier offset were used to image all FS cells. Image stacks were reconstructed in three dimensions using a neurolucida system (MBF Bioscience). To eliminate potential variability in bouton measurements at different axonal levels, our measurements were made only from terminal axonal segments in layer IV. Boutons with diameters ≥ 0.2 μm were identified and counted by a blinded observer. Bouton density per μm of axonal length was calculated in the confocal sections.

Electrophysiological data acquisition and analysis

Clampex 10 and Clampfit 10 were used for data collection and analysis, respectively. Series resistance was monitored but not compensated during the recording of either control or experimental groups. Analysis excluded IPSCs obtained with series resistances >30 MΩ, or with series resistance changes > 20%. The mean series resistance of all analyzed postsynaptic cells was 19.5 ± 0.6 MΩ (n = 64). Unitary IPSCs (including quantal events obtained with 0.5 Ca^{2+} / 3.5 Mg^{2+} - ACSF) were filtered at 2 KHz for analysis. A number of parameters of uIPSCs were measured including 1) synaptic failures: responses in which uIPSC amplitude was < 2x RMS of noise level; 2) synaptic strength: average amplitude of the uIPSCs, including synaptic transmission failures; 3) synaptic potency: average amplitudes of the uIPSCs, excluding failures; 4) coefficient of variation (CV): variance of basal noise subtracted from variance of uIPSCs; 5) synaptic latency: time from the peak of the presynaptic escape action currents to 10% amplitude of postsynaptic uIPSCs; 6) kinetics of uIPSCs: 10 - 90% rise time and 90 – 10% decay time; 7) paired pulse ratio (PPR): the ratio of the amplitude of the second (R2) to that of the first (R1) response to two consecutive presynaptic FS action currents at an interstimulus interval of 50 ms and repetition rate of 0.2 Hz. In PPR experiments, we calculated the correlation coefficient between amplitudes of two uIPSCs evoked by paired presynaptic stimulation to test whether the amplitude R2 was dependent on prior release (Xiang et al., 2002). Individual uIPSCs for measurements of synaptic strength, CV, failure rate and kinetics, were evoked at 0.33 Hz. Forty-215 (65 ± 4, n = 64) sweeps were collected to calculate synaptic failure rate; 21-100 (53 ± 3, n = 64) successful uIPSCs were selected to measure synaptic potency, CV and synaptic kinetics; and 6-67 (25 ± 1, n = 62) successful responses to paired presynaptic escape action currents were averaged to measure PPR. Except for calculation of failure rate and synaptic strength, the measurement of the other parameters excluded sweeps containing synaptic failures. The derivative of the digitally filtered current traces was used as a trigger (Ulrich and Huguenard, 1996) to detect asynchronous presumed quantal IPSCs activated by trains of presynaptic action currents. Statistical significance was determined using student *t*-test, unless otherwise noted. Data are presented as mean ± SEM.

Results

We chose to do this study in layer IV because previous experiments showed a very low “hit rate” for FS-RS cells in layer V (Xiang et al., 2002), while other groups have shown a much higher incidence of synaptically coupled FS-RS pairs in layer IV (Gibson et al., 1999). Also, from previous data, we know that the hyperexcitability is present in layer IV as well as IV (Hoffman et al., 1994). We initially determined that epileptiform activity was also present in layer IV of barrel cortex, where our paired recordings were obtained in the current experiments. Field potential recordings in layer IV of UC barrel cortex showed the same type of spontaneous and evoked, prolonged, polyphasic activities as previously reported, accompanied by polysynaptic all-or-none neuronal bursts of excitatory currents (not shown). As the recordings below were done with excitation blocked, these bursts did not interfere with the assessment of unitary IPSCs in the current experiments.

All paired recordings were obtained from neurons with intersomatic distances of < 60 μm, located within individual barrels from slices of control and injured barrel cortex of young adult rats (e.g. Fig. 1B). Barrels were identified as structures with a bright hollow center surrounded by dark septal boundaries (Feldmeyer et al., 2005) (Fig 1A). Unitary IPSCs were evoked in paired recordings involving two different postsynaptic targets of FS cells: FS-RS (21 pairs in control, 26 in UC) and FS-FS (7 pairs in control, 10 in UC). Evoked synaptic responses were blocked by adding drops of gabazine (10mM) directly to the bath (n = 6; Fig. 2), verifying the GABAergic nature of the neurotransmission. In 4 control pairs, the uIPSC were evoked by both action currents or action potentials in the presynaptic FS cell, and

uIPSC properties including amplitude, CV and PPR were not significantly different (Fig. S1).

Membrane properties of FS cells

Cortical injury might alter the membrane properties of interneurons as it does in pyramidal cells in neocortex (Prince and Tseng, 1993; Tseng and Prince, 1996), and GABAergic cells in hippocampus (Ross and Soltesz, 2000) and spinal cord (Dougherty and Hochman, 2008). Prior to examining synaptic properties of FS cells, we evaluated their membrane excitability using four parameters. Membrane input resistance (Rn) of FS cells was not altered significantly by the cortical injury (113.3 ± 5.3 MΩ in UC, n = 40, vs. 106.8 ± 6.5 MΩ in control, n = 29, $P = 0.43$; Fig. 3A, D). There was also no substantial change in spike half-width of FS cells between UC and control (0.31 ± 0.01 ms in UC, n = 40, vs. 0.33 ± 0.02 ms control, n = 29, $P = 0.59$; Fig. 3B, E). Neither the AP amplitude of FS cells, measured between AP threshold and peak, nor their AP after-hyperpolarization (AHP), measured from resting membrane potential to peak of the AHP, was significantly altered in UC vs. control pairs (AP amplitude in UC = 65.0 ± 2.0 mV, n = 40; in control = 61.3 ± 2.0 mV, n = 29; AHP amplitude in UC = 2.9 ± 0.8 mV, n = 40; in control = 1.1 ± 1.1 mV, n = 29, $P \geq 0.2$). Resting membrane potentials were significantly lower in UC FS cells (-66.8 ± 0.5 mV, n = 40) vs. controls (-64.8 ± 0.6 mV, n = 29) ($P = 0.008$). Alterations in spike frequency adaptation, which occur in layer V pyramidal neurons of partially isolated cortex (Prince and Tseng, 1993) and axotomized corticospinal cells (Tseng and Prince, 1996), were assessed in FS cells by measuring the spike frequency adaptation ratio during ~110 Hz trains of APs evoked by direct depolarizing pulses (Methods). At this frequency, activation of autaptic currents, found in a high percentage of FS cells (Bacci et al., 2003a), would not be expected to alter precise spike-timing (Bacci and Huguenard, 2006). Inspection of evoked AP trains did not reveal any significant differences in frequency adaptation ratios in UC versus control FS cells (0.60 ± 0.02, n = 40 vs. 0.55 ± 0.02, n = 29, respectively, $P = 0.13$; Fig.3C, F).

Decreased FS cell-mediated postsynaptic inhibition in excitatory principal neurons

Excitatory neurons in barrels include both spiny stellate and pyramidal cells (Cowan and Stricker 2004; Feldmeyer et al., 1999). The firing pattern and parameters of APs in these cells are significantly different from those of FS cells in that they fire an initial spike doublet at the onset of the depolarizing pulse followed by spike frequency adaptation (Fig. 1D). However it is difficult to distinguish between spiny stellate cells and pyramidal cells based only on electrophysiological properties (Cowan and Stricker, 2004). Because post-hoc analysis of biocytin-filled cells was not always sufficient to distinguish between these two excitatory cell types, we combined them in the analysis below as “RS” cells. We detected unitary synaptic connections in 26 of 43 and 33 of 53 recorded FS- RS pairs in control and UC slices, respectively. Thus, the yield of connected pairs in dual recordings (~60%) was not different in the control vs. UC tissue. Although there was occasional loss of either the FS or RS whole cell recording, the properties of inhibitory synaptic transmission were successfully quantified in 21 control and 26 UC synaptically-coupled pairs.

Several prominent differences were present in pairs from UC vs. control slices. Synaptic failures occurred in 25 of 26 FS-RS UC pairs (arrow in Fig. 4A2a, failure rate, 0.28 ± 0.04, n = 25), but in only 2 of 21 control pairs (failure rate = 0.14 ± 0.07 in the 2 pairs that had synaptic failures), suggesting that either synaptic release probability or functional synaptic contact number or both, were decreased in isolated cortex. There was also a marked decrease in the amplitude of uIPSCs in coupled pairs in UC cortex (Fig. 4A1 vs. A2) such that, under our recording conditions (postsynaptic holding potential, V_h = -70mV; E_{Cl-} = -18mV), synaptic strength (including failures) was reduced to 14% of control (35.4 ± 5.4 pA in UC vs. 245.6 ± 34.0 pA in control, n = 26 and 21 respectively, $P < 0.001$; Fig. 4B).

Similarly, the synaptic potency (i.e. average peak amplitude of uIPSCs, excluding synaptic failures) was decreased to 18% of control (45.1 ± 5.4 pA, n = 26 in UC vs. 246.9 ± 33.7 pA in control, n = 21, $P < 0.001$; Fig. 4C). The variability of uIPSC amplitude, reflected by the CV, was significantly increased in UC pairs (0.47 ± 0.03, n = 26) compared to control (0.29 ± 0.03, n = 21) ($P < 0.001$; Fig. 4D), consistent with a presynaptic alteration and suggesting a smaller quantal content in FS inhibitory terminals of the chronically epileptogenic cortex (Faber and Korn, 1991; Gibson et al., 2009). The ratio of postsynaptic RS response amplitudes (R2/R1) to 2 consecutive FS action currents with inter-spike interval of 50 ms was used to assess the PPR as an index of synaptic release probability (Lisman et al., 2007; Markram et al., 1998; Zucker and Regehr, 2002). There was an increase in the PPR for uIPSCs in UC slices (0.92 ± 0.03, n = 24 in UC vs. 0.84 ± 0.02, n = 0.21 in control; $P < 0.05$; Fig. 4E, 5A), suggesting a decreased presynaptic release probability in UC slices compared to control.

In contrast to the evident modification in presynaptic machinery, we did not find significant changes in 90-10% decay times of uIPSCs in RS cells of UC vs. control cortex ($P = 0.30$) (Table 1), suggesting that the subunit composition of postsynaptic GABAergic receptors was not significantly altered by the partial isolation, in contrast to the changes reported in dentate granule cells of the post-status epilepticus model (Brooks-Kayal et al., 1998; Schwarzer et al., 1997) and human epilepsy (Brooks-Kayal et al., 1999). In addition, uIPSCs in UC and control pairs had comparable 10-90% rise times ($P = 0.75$) (Table 1), indicating similar somatodendritic targeting. The amplitudes of the two uIPSCs evoked by the paired presynaptic stimulation (Fig. 5A) were normalized to the average of the 1st response (Fig. 5B) for both control and UC and the correlation coefficient for each connected pair was calculated (Fig. 5C). The vast majority of both control and UC groups (18 out of 21 pairs vs. 21 out of 24 pairs, respectively) showed no statistically significant correlation between R1 and R2 (-0.13 ± 0.06, range = -0.53 to 0.32, n= 21 in control; -0.04 ± 0.03, range = -0.24 to 0.32, n = 24 in UC) (Fig. 5C), indicating use-independent synaptic release in both UC and control groups. These results are consistent with those of previous studies (Hanse and Gustafsson, 2002; Xiang et al., 2002). There was also no prominent difference in synaptic latencies between UC and control uIPSCs ($P = 0.52$) (Table 1).

Impaired synaptic transmission at FS-FS synapses

The above results, showing remarkably decreased inhibitory transmission from FS axons onto RS neurons, raised the question of whether this effect was target-specific (Scanziani et al., 1998), or also involved other known FS cell contacts (Bacci et al., 2003b; Galarreta and Hestrin, 2002; Tamas et al., 2000). We therefore analyzed FS-FS uIPSCs. In FS-FS paired recordings from UC cortex, we also found significantly reduced uIPSC amplitudes (Fig. 6A2 vs. A1), but to lesser extent than at FS-RS synapses. In contrast to the above results in FS-RS uIPSCs, only 5 of 10 FS-FS pairs exhibited synaptic failures with a rate of 0.22 ± 0.09 (arrow in Fig. 6A2). There were no failures in control FS-FS pairs (n = 7; Fig.6A1). In isolated cortex, synaptic strength (including synaptic failures) in FS cells (92.2 ± 19.1 pA, n = 10) was significantly decreased to 35% of the control value (260.2 ± 60.3 pA, n = 7) ($P < 0.05$; Fig. 6B). As shown in Fig. 6C, there was a similar reduction in synaptic potency in UC pairs (97.8 ± 18.5 pA, n = 10 vs. 260.2 ± 60.3 pA in control, n = 7) ($P < 0.05$). A larger C.V. was also found in FS-FS UC pairs than in control (0.37 ± 0.02, n = 10 vs. 0.24 ± 0.03, n = 7 in control) ($P < 0.01$; Fig. 6D), again suggesting a presynaptic defect. The relatively larger PPR in UC pairs (0.91 ± 0.09, n = 10) compared to controls (0.78 ± 0.03, n = 7), did not reach statistical significance ($P = 0.18$; Fig. 6E). As in the case of FS-RS uIPSCs, 90-10% decay times, 10-90% rise times and synaptic latencies of uIPSCs in FS cells were not significantly altered ($P = 0.64$, 0.35 and 0.97, respectively) (Table 1).

Quantal size at FS-to-RS synapses

According to the theory of quantal synaptic transmission, synaptic strength is the product of three parameters: number of synaptic contacts (n), probability of synaptic release (Pr), and quantal size (q). To determine whether changes in quantal size might contribute to the reductions in uIPSC amplitude (or potency), we performed two series of experiments and quantified quantal events evoked by asynchronous release and quantal release occurring in low calcium extracellular perfusate. First, we measured asynchronous (a)IPSCs that are presumed to be a consequence of quantal release (Manseau et al., 2010; Morishita and Alger, 1997). Directly evoked high frequency trains of action currents in layer IV FS cells bathed in ACSF with strontium were followed by high frequency aIPSCs (Gibson et al., 2009; Morishita and Alger, 1997; Xiang et al., 2002) at both autapses (Fig. 7A) and FS-RS synapses (Fig. 7B), similar to those found in layer V neocortical FS cells (Manseau et al., 2010). A period of relatively high frequency aIPSCs lasting 300 ms followed the action current trains, allowing amplitude measurement (dashed rectangles in Fig. 7B). The delay in selection of the time window in control vs. UC was caused by the longer asynchronous release and the resulting longer post-stimulus temporal summation in control pairs, likely due to the larger number of functional synaptic contacts and higher Pr in control pairs, as suggested by the present study. Due to the difficulty in completely eliminating contamination of aIPSCs by spontaneous IPSCs, only recorded pairs with a correction factor (cf, see Methods) less than one third (28 ± 2%, n = 10 pairs) were analyzed and included in the following comparison. Analysis of aIPSCs in postsynaptic RS cells of 10 pairs (n = 190 ± 27 events, range = 65-310 aIPSCs/RS cell) indicated that there was no significant difference in aIPSC amplitude between UC postsynaptic RS cells (17.7 ± 3.4 pA, n = 5 pairs) compared to control RS cells (23.4 ± 3.4 pA, n = 5 pairs) ($P = 0.28$; Fig. 7G).

In a second experiment, we perfused slices with low Ca^{2+} / high Mg^{2+} - ACSF to detect presumed quantal release (Gibson et al., 2009; Zhang and Buckmaster, 2009). After synaptic failure rates for uIPSCs evoked by escape action currents in FS cells were greater than 80% in postsynaptic RS neurons, 8-18 presumed quantal events were collected for each of 5 control and 4 UC FS-RS connections prior to 100% synaptic failure rate (Fig. 7E, F). There was no significant differences in mean amplitudes of presumed quantal IPSCs between UC (26.3 ± 3.7 μA, n = 5) and control pairs (23.0 ± 6.0 μA, n = 4) ($P = 0.68$) (Fig. 7H). The apparent variation in quantal amplitudes was likely attributable to variation in transmitter content within single vesicles (Frerking et al., 1995) instead of differences in number of postsynaptic $GABA_A$ receptors (Perrais and Ropert, 1999).

The quantal sizes revealed by the above two approaches were similar and the quantal size of control connections was similar to the values obtained at FS-RS synapses in layer V of rat visual cortex (Xiang et al., 2002). From the above average amplitudes of uIPSCs for UC and control groups, excluding failures (45.1 ± 5.4 pA and 246.9 ± 33.7 pA, respectively, see above), and the estimates of average quantal size from the above two sets of experiments (20.4 pA in UC and 24.9 pA for control), we estimate that one action current in a presynaptic FS cell activated vesicle release at, on average, 2.2 ± 0.3 release sites in UC slices and 9.9 ± 1.4 in control tissue, values consistent with the higher failure rate and the increased CV for uIPSCs in isolated cortex (Faber and Korn, 1991; Gibson et al., 2009). These approximations assume that multivesicular release is not a common feature of inhibitory transmission under physiologically relevant divalent cation concentrations (Biro et al., 2006).

Presynaptic FS bouton numbers

The striking four-fold reduction in quantal content (2.5 vs. 10.6 estimated synapses in UC slices vs. controls, as shown above), was difficult to explain solely by the relatively modest

12% increase in PPR (Fig. 4E). A reduced number of synaptic contacts presynaptically formed by FS cells might also contribute to the reduced inhibition mediated by FS cells that was also in line with an increase in CV for uIPSCs. To indirectly assess this issue, we analyzed axonal terminals in FS cells with well-filled axonal arbors and high quality biocytin staining. We found no obvious changes in the predominant pattern of FS axon distribution in UC vs. control FS cells. Axons of almost all of the analyzed 4 control and 4 UC cells (7 of 8) emerged either from the upper pole (pial side) of the soma or from ascending dendritic trunks and headed towards layer II/III. All of the 8 FS cells made at least one main recurrent axonal loop towards soma and the vast majority of the axonal arborization of all 8 FS cells distributed in layer IV to form a tight cluster that appeared restricted to single barrels. To eliminate potential variability in bouton measurements at different axonal levels, our measurements were made only from terminal axonal segments in layer IV.

Three terminal axonal segments from each of 4 UC and 4 control FS cells were selected randomly and imaged in each neuron (see Methods). VGAT immunocytochemistry was used in some cells to confirm that axonal swellings were GABAergic boutons (not shown). The total axonal length measured was 827.2 μm in control and 967.3 μm in UC cells. Bouton density was calculated as bouton number/μm. These measurements showed that UC FS cells had occasional long gaps between boutons (big arrows in Fig. 8A) and significantly lower bouton density (0.28 ± 0.01 / μm in 4 UC cells vs. 0.34 ± 0.04 / μm in 4 control cells; $P < 0.05$; Fig. 8B).

Discussion

The principal finding of these experiments is impaired inhibitory synaptic transmission from layer IV FS interneurons onto excitatory neurons and other FS cells in barrel cortex of the undercut model of posttraumatic neocortical epileptogenesis. This reduced efficacy of inhibition appears to be mediated by presynaptic effects at inhibitory terminals as indicated by decreased release probability, increases in CV of uIPSC amplitude, increases in synaptic failures, and a reduced number of presynaptic boutons. Further, dysfunction in the synaptic terminals of surviving FS interneurons is not target-selective (Scanziani et al., 1998), as similar, though quantitatively different decreases in uIPSCs are present at both FS-RS and FS-FS contacts. The absence of abnormalities in kinetics of uIPSCs or in quantal size indicates that postsynaptic factors do not contribute to the reduced GABAergic inhibition.

Inhibitory abnormalities in chronic epilepsy

Anatomical and electrophysiological experiments have documented a number of alterations in GABAergic interneurons and/or in postsynaptic inhibition that vary in different animal models of epileptogenesis (see references in Introduction). Depending on the location, interneuronal cell type examined and timing of the experiments in relation to the time and type of injury, interneuronal membrane properties may be unchanged (current results; Morin et al., 1998; Rempe et al., 1997) or altered significantly (Halabisky et al., 2010); uIPSC amplitude unaffected (somatostatin interneuron to granule cell synapses in Zhang et al., 2009) or markedly decreased (FS-RS uIPSCs in current results); and output from a given subtype of interneuron unaffected, increased or decreased (Cossart et al., 2001, 2005). Due to this variability and the heterogeneity of interneurons and their properties (Ascoli et al., 2008), we chose to narrow our examination of inhibitory transmission to that generated by a specific interneuronal subtype (FS cells) within a specific neocortical area (barrel cortex) in the undercut model. The paucity of large cholecystokinin (CCK)-containing, interneurons in layer IV of barrel cortex (Bodor et al., 2005), makes it unlikely that CCK cells are significantly represented in the population of FS cells recorded in the present experiments. Rather, the FS cells we recorded are likely all parvalbumin (PV)-containing inhibitory

interneurons (Kawaguchi and Kondo, 2002; Kawaguchi and Kubota, 1997; Uematsu et al., 2008). Evidence from a variety of experiments indicates that PV-containing interneurons are vulnerable to injury in chronic epileptogenic lesions in neocortex (Roper et al., 1999; Rosen et al., 1998; Silva et al., 2002; Trotter et al., 2006; Zamecnik et al., 2006) and hippocampus (Andrioli et al., 2007; Scotti et al., 1997). However, information regarding the functional properties of the surviving FS interneurons is incomplete. In epileptogenic microgyri in barrel cortex induced by neonatal focal freeze lesions, a marked reduction in uIPSCs amplitude from FS to excitatory neurons is present (Sun et al., 2005), suggesting that alterations in GABAergic inhibition mediated by FS interneurons may be common to other neocortical epileptogenic injuries. The intrinsic membrane properties of the FS cells measured in whole cell recordings from somata were unaltered in the UC cortex, as is also the case in some other models of epileptogenesis (Morin et al., 1998; Rempe et al., 1997), even though a variety of interneuronal anatomical alterations are known to occur in epileptogenic tissue (Arellano et al., 2004; Bausch, 2005; Prince et al., 2009; Zhang et al., 2009). This apparent discrepancy is likely due to the insensitivity of the somatic recordings in detecting intrinsic functional abnormalities at distant dendritic (Shah et al., 2004) and axonal sites (Grubb and Burrone, 2010).

Presynaptic abnormalities underlie reduced uIPSCs in epileptogenic cortex

Multiple mechanisms might contribute to the reduced GABA release in our experiments. GABAergic terminals possess a variety of receptors whose activation can affect transmitter release (Bacci et al., 2004; Bowery et al., 1980; Lambert and Wilson, 1993; Marsicano et al., 1999; Yamamoto et al., 2010). To significantly reduce single uIPSCs, involved receptors would have to be tonically activated. Cannabinoid CB1 receptor activation affects GABA release from some interneuronal subtypes, however FS interneurons do not have CB1 receptors on their terminals (Galarreta et al., 2008; Marsicano et al., 1999). Activation of peptidergic or $GABA_B$ presynaptic receptors would require repetitive stimulation of the interneurons (Bacci et al., 2002; Sun et al., 2003) or synchronous activation of multiple inhibitory cells (Davies et al., 1990), conditions not present in the present experiments. Also, in recent experiments it was shown that $GABA_B$ receptor blockade in UC neocortical slices had no effect on the PPR for pairs of monosynaptic IPSCs (Faria and Prince, 2010).

A potential mechanism for the shift toward facilitation in the PPR in UC cortex is decreased Ca^{2+} buffering and a resultant increase in residual Ca^{2+} in terminals (Caillard et al., 2000; Collin et al., 2005; Zucker and Regehr, 2002). The calcium binding protein, PV, is highly expressed in most FS interneurons (Celio, 1986) and PV-containing interneurons and their axon terminals in epileptogenic neocortex or hippocampus may lose or decrease their PV content (Andre et al., 2001; Roper et al., 1999; Rosen et al., 1998; Scotti et al., 1997; Wittner et al., 2001, 2005). Such changes would result in alterations in Ca^{2+} buffering and could underlie the shifts toward paired pulse facilitation (Vreugdenhil et al., 2003). However, in the present study, neurons in naïve and undercut cortex were perfused with the same intracellular solution containing calcium buffer (1.1 mM EGTA), making it unlikely that alterations in intrinsic calcium buffer underlie the changes in PPR in the injured cortex.

Assuming that PPR is a reflection of that portion of Pr mediated by calcium influx at presynaptic terminals (Lisman et al., 2007; Markram et al., 1998; Zucker and Regehr, 2002; but see Manita et al., 2007), the increase in PPR in partially isolated cortex (Fig. 4E) would most likely reflects a reduction in synaptic Pr due to alterations in calcium entry into terminals. This conclusion is supported by our observation that an elevated extracellular calcium concentration ($[Ca^{2+}]_o$) induced a reduction in PPR in the undercut model (Faria and Prince, 2010), and that PPR is dependent on $[Ca^{2+}]_o$ in other results (Fleidervish and Gutnick, 1995; Jensen et al., 1999; Kravchenko et al., 2006; Lambert and Wilson, 1994; Wilcox and Dichter, 1994). Information regarding a quantitative relationship between the

PPR and Pr at neocortical GABAergic synapses is not available. If we assume that data reported in experiments involving excitatory postsynaptic currents (EPSCs) at the calyx of Held (e.g. Oleskevich et al., 2000; Oleskovich and Walmsley, 2002) are applicable to inhibitory transmission in neocortex, there would be a roughly linear negative correlation between PPR and Pr at various concentration of calcium. Therefore, we estimate the 12% increase in PPR only reflects an ~10% decrease in Pr that could be attributable to compromised calcium entry at terminals.

Nevertheless, there is a mismatch between the four-fold reduction in quantal content (2.5 vs. 10.6 estimated synapses in UC slices vs. controls, as shown above), and the ~10% decrease in Pr. According to the theory of quantal synaptic transmission and assuming that under physiological relevant conditions, only one vesicle is released from a single release site at inhibitory synapses (Biro et al., 2006), a reduced number of functional release sites could be one of the explanations for this mismatch. This suggestion is partially supported by the analysis of biocytin-filled FS interneuronal axons that shows a 17% decrease in bouton density in FS axons of the UC cortex (Fig. 8). Results of EM studys in cat suprasylvian neocortical isolations showed decreased symmetrical synapses on pyramidal cells at the margins of the lesioned cortex (Ribak and Reiffenstein, 1982) and recent quantitative EM results in rat undercut cortex showed a ~30% reduction in somatic symmetrical synapses (J. Wenzel, P.A. Schawrtzkroin and D.A. Prince, unpublished). However, the relatively moderate reductions in Pr due to changes in calcium influx and bouton/synaptic density still cannot account for the dramatic four-fold reduction in synaptic strength (Fig 4B). Therefore, other abnormalities may also be present and affect Pr, such as defects in the presynaptic vesicle release machinery. For example, abnormal docking processes can reduce the number of functional release sites and the readily releasable vesicle pool (Weimer et al., 2003). Consequently, both the n (number of synaptic contacts) and Pr associated with readily releasable vesicle pool (Dobrunz, 2002; Dobrunz and Stevens,1997) would be reduced.

Genetically reducing the levels of SNARE proteins including syntaxin and synaptobrevin has also been shown to dampen the strength of synaptic transmission (Stewart et al., 2000). Another presynaptic mechanism for decreased uIPSC amplitude and increased failure rate might be branch point failure as described in crustaceans (Hatt and Smith, 1976), suggested in a modeling study (Lüscher and Shiner, 1990) and results of experiments in hippocampal slice culture (Debanne et al, 1997). However, calcium imaging with two-photon laser scanning microscopy has directly demonstrated that single action potentials or bursts of action potentials in layer II/III pyramidal cells reliably invade single varicosities in cortical axonal terminals, presumably presynaptic boutons, on 2^{nd}- to 4^{th}-order axonal branches that were up to 500 μm from the soma (Cox et al., 2000). The issue of whether branch point failure might occur at the finest terminal axonal branches of interneurons remains unsettled (Huguenard, 2000). We cannot completely rule out this possibility as a factor contributing to our results, although it is unlikely (e.g. Allen and Stevens, 1994).

Postsynaptic abnormalities might also account for decreases in inhibitory currents. Alterations in postsynaptic receptors that might affect IPSCs were previously reported in epileptogenic hippocampus (Brooks-Kayal et al., 1998; Gibbs, III et al., 1997). We found no changes in IPSC kinetics of uIPSCs in our experiments, suggesting that postsynaptic $GABA_A$ receptor subunit composition was not significantly altered. Absence of significant changes in quantal size makes it unlikely that a reduced number of postsynaptic receptors, or a decrease in GABA content inside single vesicles, underlies the decreases in uIPSC amplitude.

Estimates of quantal size at FS-RS synapses

Both a small decrease in mIPSCs onto hippocampal CA1 pyramidal neurons (Hirsch et al., 1999) and an increase in quantal size at basket cell to dentate granule cell synapses (Zhang and Buckmaster, 2009) have been reported in the pilocarpine model of temporal lobe epilepsy.

To estimate changes in quantal size, we took advantage of the asynchronous GABA release at FS-RS synapses that follows high frequency FS cell spiking (Manseau et al., 2010) and is thought to represent quantal release from individual release sites (Daw et al., 2009). Quantal size estimated with this method was comparable to that obtained with low Ca^{2+} / high Mg^{2+} extracellular solution, reducing concerns that the estimate based on asynchronous release might have been influenced by receptor desensitization caused by the high frequency stimulation (Bianchi and Macdonald, 2001). The comparable results obtained by these two methods also suggest that there are no differences in quantal size in reserve and readily releasable vesicle pools, which might be selectively recruited in asynchronous and synchronous release experiments. The present data on quantal events originating from FS interneurons are not directly comparable to those previously obtained in whole cell recordings from single layer V pyramidal cells in tetrodotoxin where mIPSCs presumably also included events from other presynaptic interneuron subtypes (Li and Prince 2002). Nonetheless, the mIPSC amplitude was also not significantly altered in undercut vs. control animals in the earlier experiments (Li and Prince, 2002).

Our results show that the functional properties of a major class of surviving GABAergic neurons are markedly affected by neocortical injury. Obviously, counts of GABAergic cells in epileptogenic lesions cannot detect the type of dysfunction in survivors found in these experiments. We also show that normal somatic intrinsic membrane properties can coexist with substantial functional alterations in axonal terminals. We expect that more significant alterations in interneuronal function may be present in other models where severe trauma results in more widespread and much larger lesions (Pitkanen et al., 2009) or in penetrating human traumatic brain injury (Salazar et al., 1985). Hypothesized loss of support by BDNF (Marty et al., 2000) after injury, offers a potential rationale for future antiepileptogenic therapy directed at improving interneuronal function with trophic substances (Li et al., 2011).

The net effects of the reductions in GABAergic inhibition resulting from the above abnormalities in FS interneurons are difficult to predict, however the large decreases in inhibitory transmission reported here would be expected to have epileptogenic effects. Reductions in the perisomatic / proximal inhibition, normally generated by FS cells, will limit their function to control spike output of excitatory cells through inhibitory and shunting effects (Miles et al., 1996; Mitchell and Silver, 2003). Even a small generalized reduction in GABAergic inhibition, induced pharmacologically, results in abnormal propagation of cortical activity and epileptiform activity in naïve neocortical slices (Chagnac-Amitai and Connors, 1989). In a network with injury-induced increased recurrent excitatory connectivity, as is present in the UC cortex (Jin et al., 2006; Salin et al., 1995), such marked disinhibition would be even more likely to contribute to epileptiform activity (Traub et al., 1989). The decreased inhibition at FS-FS interneuronal synapses (e.g. Fig. 6), though not as marked as at FS-RS connections, might be hypothesized to increase interneuronal output. However, such an effect would be muted by the marked alterations at presynaptic terminals of the disinhibited FS cells.

Neocortical neurons receive inhibitory inputs from a variety of interneurons (Bacci et al., 2003b; Beierlein et al., 2003) that likely have varying susceptibility to injury (Cossart et al., 2001) and to genetic defects (Gibson et al., 2009). Therefore it is unclear whether inhibitory

transmission from other subclasses of neocortical interneurons is affected in this model of posttraumatic epileptogenesis. Previous data from pharmacologically isolated monosynaptic IPSCs on layer V pyramidal cells and FS interneurons are consistent with the present results in that they showed decreased amplitude, increased failures, and increased PPR for IPSCs in both cell types (Faria and Prince, 2010). However, analysis of unitary inhibitory output of additional subclasses of neocortical interneurons, e.g. somatostatin-containing, low threshold spiking cells, will be required to determine the extent to which they share the above defects in GABA release.

Supplementary Material

Refer to Web version on PubMed Central for supplementary material.

Acknowledgments

We thank Ms. Isabel Parada for assistance in immunocytochemical experiments and Professor Michael Gutnick for helpful suggestions. This work was supported by the National Institutes of Health grants NS012151 and NS039579 from National Institute of Neurological Disorders and Stroke.

References

Allen C, Stevens CF. An evaluation of causes for unreliability of synaptic transmission. Proc Natl Acad Sci U S A. 1994; 91:10380–3. [PubMed: 7937958]

Andre V, Marescaux C, Nehlig A, Fritschy JM. Alterations of hippocampal GABAergic system contribute to development of spontaneous recurrent seizures in the rat lithium-pilocarpine model of temporal lobe epilepsy. Hippocampus. 2001; 11:452–468. [PubMed: 11530850]

Andrioli A, Alonso-Nanclares L, Arellano JI, DeFelipe J. Quantitative analysis of parvalbumin-immunoreactive cells in the human epileptic hippocampus. Neuroscience. 2007; 149:131–143. [PubMed: 17850980]

Annegers JF, Hauser WA, Coan SP, Rocca WA. A population-based study of seizures after traumatic brain injuries. N Engl J Med. 1998; 338:20–4. [PubMed: 9414327]

Arellano JI, Munoz A, Ballesteros-Yanez I, Sola RG, DeFelipe J. Histopathology and reorganization of chandelier cells in the human epileptic sclerotic hippocampus. Brain. 2004; 127:45–64. [PubMed: 14534159]

Ascoli GA, Alonso-Nanclares L, Anderson SA, Barrionuevo G, Benavides-Piccione R, Burkhalter A, Buzsaki G, Cauli B, DeFelipe J, Fairen A. Petilla terminology: nomenclature of features of GABAergic interneurons of the cerebral cortex. Nat Rev Neurosci. 2008; 9:557–568. [PubMed: 18568015]

Avramescu S, Timofeev I. Synaptic Strength Modulation after Cortical Trauma: A Role in Epileptogenesis. J Neurosci. 2008; 28:6760–6772. [PubMed: 18596152]

Bacci A, Huguenard JR. Enhancement of spike-timing precision by autaptic transmission in neocortical inhibitory interneurons. Neuron. 2006; 49:119–130. [PubMed: 16387644]

Bacci A, Huguenard JR, Prince DA. Differential modulation of synaptic transmission by neuropeptide Y in rat neocortical neurons. Proc Natl Acad Sci U S A. 2002; 99:17125–17130. [PubMed: 12482942]

Bacci A, Huguenard JR, Prince DA. Functional autaptic neurotransmission in fast-spiking interneurons: a novel form of feedback inhibition in the neocortex. J Neurosci. 2003a; 23:859–866. [PubMed: 12574414]

Bacci A, Rudolph U, Huguenard JR, Prince DA. Major differences in inhibitory synaptic transmission onto two neocortical interneuron subclasses. J Neurosci. 2003b; 23:9664–9674. [PubMed: 14573546]

Bacci A, Huguenard JR, Prince DA. Long-lasting self-inhibition of neocortical interneurons mediated by endocannabinoids. Nature. 2004; 431:312–316. [PubMed: 15372034]

Bausch SB. Axonal sprouting of GABAergic interneurons in temporal lobe epilepsy. Epilepsy Behav. 2005; 7:390–400. [PubMed: 16198153]

Beierlein M, Gibson JR, Connors BW. Two Dynamically Distinct Inhibitory Networks in Layer 4 of the Neocortex. Journal of Neurophysiology. 2003; 90:2987–3000. [PubMed: 12815025]

Bernard C, Cossart R, Hirsch JC, Esclapez M, Ben Ari Y. What is GABAergic inhibition? How is it modified in epilepsy? Epilepsia. 2000; 41(Suppl 6):S90–S95. [PubMed: 10999527]

Bianchi MT, Macdonald RL. Agonist Trapping by GABAA Receptor Channels. J Neurosci. 2001; 21:9083–9091. [PubMed: 11717341]

Biro AA, Holderith NB, Nusser Z. Release probability-dependent scaling of the postsynaptic responses at single hippocampal GABAergic synapses. J Neurosci. 2006; 26:12487–12496. [PubMed: 17135411]

Bodor AL, Katona I, Nyiri G, Mackie K, Ledent C, Hajos N, Freund TF. Endocannabinoid signaling in rat somatosensory cortex: laminar differences and involvement of specific interneuron types. J Neurosci. 2005; 25:6845–6856. [PubMed: 16033894]

Bowery NG, Hill DR, Hudson AL, Doble A, Middlemiss DN, Shaw J, Turnbull M. (-)Baclofen decreases neurotransmitter release in the mammalian CNS by an action at a novel GABA receptor. Nature. 1980; 283:92–4. [PubMed: 6243177]

Brooks-Kayal AR, Shumate MD, Jin H, Lin DD, Rikhter TY, Holloway KL, Coulter DA. Human neuronal gamma-aminobutyric acid(A) receptors: coordinated subunit mRNA expression and functional correlates in individual dentate granule cells. J Neurosci. 1999; 19:8312–8318. [PubMed: 10493732]

Brooks-Kayal AR, Shumate MD, Jin H, Rikhter TY, Coulter DA. Selective changes in single cell GABA(A) receptor subunit expression and function in temporal lobe epilepsy. Nat Med. 1998; 4:1166–1172. [PubMed: 9771750]

Buckmaster PS, Dudek FE. Neuron loss, granule cell axon reorganization, and functional changes in the dentate gyrus of epileptic kainate-treated rats. J Comp Neurol. 1997; 385:385–404. [PubMed: 9300766]

Buckmaster PS, Jongen-Relo AL. Highly Specific Neuron Loss Preserves Lateral Inhibitory Circuits in the Dentate Gyrus of Kainate-Induced Epileptic Rats. J Neurosci. 1999; 19:9519–9529. [PubMed: 10531454]

Caillard O, Moreno H, Schwaller B, Llano I, Celio MR, Marty A. Role of the calcium-binding protein parvalbumin in short-term synaptic plasticity. Proc Natl Acad Sci U S A. 2000; 97:13372–13377. [PubMed: 11069288]

Celio MR. Parvalbumin in most gamma-aminobutyric acid-containing neurons of the rat cerebral cortex. Science. 1986; 231:995–997. [PubMed: 3945815]

Chagnac-Amitai Y, Connors BW. Horizontal spread of synchronized activity in neocortex and its control by GABA-mediated inhibition. J Neurophysiol. 1989; 61:747–58. [PubMed: 2542471]

Collin T, Marty A, Llano I. Presynaptic calcium stores and synaptic transmission. Curr Opin Neurobiol. 2005; 15:275–281. [PubMed: 15919193]

Cossart R, Bernard C, Ben Ari Y. Multiple facets of GABAergic neurons and synapses: multiple fates of GABA signalling in epilepsies. Trends Neurosci. 2005; 28:108–115. [PubMed: 15667934]

Cossart R, Dinocourt C, Hirsch JC, Merchan-Perez A, De Felipe J, Ben Ari Y, Esclapez M, Bernard C. Dendritic but not somatic GABAergic inhibition is decreased in experimental epilepsy. Nat Neurosci. 2001; 4:52–62. [PubMed: 11135645]

Cowan AI, Stricker C. Functional connectivity in layer IV local excitatory circuits of rat somatosensory cortex. J Neurophysiol. 2004; 92:2137–2150. [PubMed: 15201316]

Cox CL, Denk W, Tank DW, Svoboda K. Action potentials reliably invade axonal arbors of rat neocortical neurons. Proc Natl Acad Sci U S A. 2000; 97:9724–8. [PubMed: 10931955]

D'Ambrosio R, Fairbanks JP, Fender JS, Born DE, Doyle DL, Miller JW. Post-traumatic epilepsy following fluid percussion injury in the rat. Brain. 2004; 127:304–314. [PubMed: 14607786]

Davies CH, Davies SN, Collingridge GL. Paired-pulse depression of monosynaptic GABA-mediated inhibitory postsynaptic responses in rat hippocampus. J Physiol. 1990; 424:513–531. [PubMed: 2167975]

Daw MI, Tricoire L, Erdelyi F, Szabo G, McBain CJ. Asynchronous transmitter release from cholecystokinin-containing inhibitory interneurons is widespread and target-cell independent. J Neurosci. 2009; 29:11112–11122. [PubMed: 19741117]

Debanne D, Guerineau NC, Gahwiler BH, Thompson SM. Action-potential propagation gated by an axonal I(A)-like K+ conductance in hippocampus. Nature. 1997; 389:286–289. [PubMed: 9305843]

Dinocourt C, Petanjek Z, Freund TF, Ben Ari Y, Esclapez M. Loss of interneurons innervating pyramidal cell dendrites and axon initial segments in the CA1 region of the hippocampus following pilocarpine-induced seizures. J Comp Neurol. 2003; 459:407–425. [PubMed: 12687707]

Dobrunz LE. Release probability is regulated by the size of the readily releasable vesicle pool at excitatory synapses in hippocampus. Int J Dev Neurosci. 2002; 20:225–236. [PubMed: 12175858]

Dobrunz LE, Stevens CF. Heterogeneity of release probability, facilitation, and depletion at central synapses. Neuron. 1997; 18:995–1008. [PubMed: 9208866]

Dougherty KJ, Hochman S. Spinal cord injury causes plasticity in a subpopulation of lamina I GABAergic interneurons. J Neurophysiol. 2008; 100:212–223. [PubMed: 18480373]

ECHLIN FA. The supersensitivity of chronically “isolated” cerebral cortex as a mechanism in focal epilepsy. Electroencephalogr Clin Neurophysiol. 1959; 11:697–722. [PubMed: 13819191]

Elfant D, Pal BZ, Emptage N, Capogna M. Specific inhibitory synapses shift the balance from feedforward to feedback inhibition of hippocampal CA1 pyramidal cells. Eur J Neurosci. 2008; 27:104–113. [PubMed: 18184315]

Faber DS, Korn H. Applicability of the coefficient of variation method for analyzing synaptic plasticity. Biophys J. 1991; 60:1288–1294. [PubMed: 1684726]

Faria LC, Prince DA. Presynaptic inhibitory terminals are functionally abnormal in a rat model of posttraumatic epilepsy. J Neurophysiol. 2010; 104:280–90. [PubMed: 20484536]

Feldmeyer D, Egger V, Lubke J, Sakmann B. Reliable synaptic connections between pairs of excitatory layer 4 neurones within a single ‘barrel’ of developing rat somatosensory cortex. J Physiol. 1999; 521(Pt 1):169–190. [PubMed: 10562343]

Feldmeyer D, Roth A, Sakmann B. Monosynaptic connections between pairs of spiny stellate cells in layer 4 and pyramidal cells in layer 5A indicate that lemniscal and paralemniscal afferent pathways converge in the infragranular somatosensory cortex. J Neurosci. 2005; 25:3423–3431. [PubMed: 15800197]

Fleidervish IA, Gutnick MJ. Paired-pulse facilitation of IPSCs in slices of immature and mature mouse somatosensory neocortex. J Neurophysiol. 1995; 73:2591–2595. [PubMed: 7666166]

Galante M, Marty A. Presynaptic ryanodine-sensitive calcium stores contribute to evoked neurotransmitter release at the basket cell-Purkinje cell synapse. J Neurosci. 2003; 23:11229–11234. [PubMed: 14657182]

Galarreta M, Erdelyi F, Szabo G, Hestrin S. Cannabinoid sensitivity and synaptic properties of 2 GABAergic networks in the neocortex. Cereb Cortex. 2008; 18:2296–2305. [PubMed: 18203691]

Galarreta M, Hestrin S. Electrical and chemical synapses among parvalbumin fast-spiking GABAergic interneurons in adult mouse neocortex. Proc Natl Acad Sci U S A. 2002; 99:12438–12443. [PubMed: 12213962]

Gibbs JW III, Shumate MD, Coulter DA. Differential epilepsy-associated alterations in postsynaptic GABA(A) receptor function in dentate granule and CA1 neurons. J Neurophysiol. 1997; 77:1924–1938. [PubMed: 9114245]

Gibson JR, Beierlein M, Connors BW. Two networks of electrically coupled inhibitory neurons in neocortex. Nature. 1999; 402:75–79. [PubMed: 10573419]

Gibson JR, Huber KM, Sudhof TC. Neuroligin-2 deletion selectively decreases inhibitory synaptic transmission originating from fast-spiking but not from somatostatin-positive interneurons. J Neurosci. 2009; 29:13883–13897. [PubMed: 19889999]

Graber KD, Prince DA. A critical period for prevention of posttraumatic neocortical hyperexcitability in rats. Ann Neurol. 2004; 55:860–870. [PubMed: 15174021]

Graber, KD.; Prince, DA. Chronic partial cortical isolation.. In: Pitkanen, A.; Schwartzkroin, P.; Moshe, S., editors. Models of Seizures and Epilepsy. Elsevier Academic Press; San Diego: 2006. p. 477-493.

Grubb MS, Burrone J. Activity-dependent relocation of the axon initial segment fine-tunes neuronal excitability. Nature. 2010; 465:1070–1074. [PubMed: 20543823]

Halabisky B, Parada I, Buckmaster PS, Prince DA. Excitatory input onto hilar somatostatin interneurons is increased in a chronic model of epilepsy. J Neurophysiol. 2010; 104:2214–2223. [PubMed: 20631216]

Hanse E, Gustafsson B. Release dependence to a paired stimulus at a synaptic release site with a small variable pool of immediately releasable vesicles. J Neurosci. 2002; 22:4381–7. [PubMed: 12040044]

Hatt H, Smith DO. Synaptic depression related to presynaptic axon conduction block. J Physiol. 1976; 259:367–93. [PubMed: 182964]

Hirsch JC, Agassandian C, Merchan-Perez A, Ben Ari Y, DeFelipe J, Esclapez M, Bernard C. Deficit of quantal release of GABA in experimental models of temporal lobe epilepsy. Nat Neurosci. 1999; 2:499–500. [PubMed: 10448211]

Hoffman SN, Salin PA, Prince DA. Chronic neocortical epileptogenesis in vitro. J Neurophysiol. 1994; 71:1762–1773. [PubMed: 8064347]

Houser CR, Esclapez M. Downregulation of the alpha5 subunit of the GABA(A) receptor in the pilocarpine model of temporal lobe epilepsy. Hippocampus. 2003; 13:633–645. [PubMed: 12921352]

Huguenard JR. Reliability of axonal propagation: the spike doesn't stop here. Proc Natl Acad Sci U S A. 2000; 97:9349–50. [PubMed: 10944204]

Jensen K, Lambert JD, Jensen MS. Activity-dependent depression of GABAergic IPSCs in cultured hippocampal neurons. J Neurophysiol. 1999; 82:42–49. [PubMed: 10400933]

Jin X, Huguenard JR, Prince DA. Impaired Cl- extrusion in layer V pyramidal neurons of chronically injured epileptogenic neocortex. J Neurophysiol. 2005; 93:2117–2126. [PubMed: 15774713]

Kawaguchi Y, Kondo S. Parvalbumin, somatostatin and cholecystokinin as chemical markers for specific GABAergic interneuron types in the rat frontal cortex. J Neurocytol. 2002; 31:277–287. [PubMed: 12815247]

Kawaguchi Y, Kubota Y. GABAergic cell subtypes and their synaptic connections in rat frontal cortex. Cereb Cortex. 1997; 7:476–486. [PubMed: 9276173]

Kobayashi M, Buckmaster PS. Reduced inhibition of dentate granule cells in a model of temporal lobe epilepsy. J Neurosci. 2003; 23:2440–2452. [PubMed: 12657704]

Kravchenko MO, Moskalyuk AO, Fedulova SA, Veselovsky NS. Calcium-dependent changes of paired-pulse modulation at single GABAergic synapses. Neurosci Lett. 2006; 395:133–137. [PubMed: 16321469]

Kumar SS, Buckmaster PS. Hyperexcitability, interneurons, and loss of GABAergic synapses in entorhinal cortex in a model of temporal lobe epilepsy. J Neurosci. 2006; 26:4613–4623. [PubMed: 16641241]

Lambert NA, Wilson WA. Heterogeneity in presynaptic regulation of GABA release from hippocampal inhibitory neurons. J Physiol. 1993; 11:1057–1067.

Lambert NA, Wilson WA. Temporally distinct mechanisms of use-dependent depression at inhibitory synapses in the rat hippocampus in vitro. J Neurophysiol. 1994; 72:121–130. [PubMed: 7964997]

Li H, McDonald W, Parada I, Faria L, Graber K, Takahashi DK, Ma Y, Prince D. Targets for preventing epilepsy following cortical injury. Neurosci Lett. 2011; 497:172–176. [PubMed: 21354270]

Li H, Prince DA. Synaptic Activity in Chronically Injured, Epileptogenic Sensory-Motor Neocortex. Journal of Neurophysiology. 2002; 88:2–12. [PubMed: 12091528]

Lisman JE, Raghavachari S, Tsien RW. The sequence of events that underlie quantal transmission at central glutamatergic synapses. Nat Rev Neurosci. 2007; 8:597–609. [PubMed: 17637801]

Loup F, Wieser HG, Yonekawa Y, Aguzzi A, Fritschy JM. Selective alterations in GABAA receptor subtypes in human temporal lobe epilepsy. J Neurosci. 2000; 20:5401–5419. [PubMed: 10884325]

Lowenstein DH, Thomas MJ, Smith DH, McIntosh TK. Selective vulnerability of dentate hilar neurons following traumatic brain injury: a potential mechanistic link between head trauma and disorders of the hippocampus. J Neurosci. 1992; 12:4846–4853. [PubMed: 1464770]

Luhmann HJ, Mittmann T, van Luijtelaar G, Heinemann U. Impairment of intracortical GABAergic inhibition in a rat model of absence epilepsy. Epilepsy Res. 1995; 22:43–51. [PubMed: 8565966]

Lüscher HR, Shiner JS. Simulation of action potential propagation in complex terminal arborizations. Biophys J. 1990; 58:1389–99. [PubMed: 2275959]

Maccaferri G, Roberts JD, Szucs P, Cottingham CA, Somogyi P. Cell surface domain specific postsynaptic currents evoked by identified GABAergic neurones in rat hippocampus in vitro. J Physiol. 2000; 524(Pt 1):91–116. [PubMed: 10747186]

Magloczky Z, Freund TF. Impaired and repaired inhibitory circuits in the epileptic human hippocampus. Trends Neurosci. 2005; 28:334–340. [PubMed: 15927690]

Manita S, Suzuki T, Inoue M, Kudo Y, Miyakawa H. Paired-pulse ratio of synaptically induced transporter currents at hippocampal CA1 synapses is not related to release probability. Brain Res. 2007; 1154:71–79. [PubMed: 17482582]

Manseau F, Marinelli S, Mendez P, Schwaller B, Prince DA, Huguenard JR, Bacci A. Desynchronization of neocortical networks by asynchronous release of GABA at autaptic and synaptic contacts from fast-spiking interneurons. PLoS Biol. 2010; 8(9)

Marco P, Sola RG, Cajal S, DeFelipe J. Loss of inhibitory synapses on the soma and axon initial segment of pyramidal cells in human epileptic peritumoural neocortex: implications for epilepsy. Brain Res Bull. 1997; 44:47–66. [PubMed: 9288831]

Marco P, Sola RG, Pulido P, Alijarde MT, Sanchez A, Cajal S, DeFelipe J. Inhibitory neurons in the human epileptogenic temporal neocortex. An immunocytochemical study. Brain. 1996; 119(Pt 4): 1327–1347. [PubMed: 8813295]

Markram H, Pikus D, Gupta A, Tsodyks M. Potential for multiple mechanisms, phenomena and algorithms for synaptic plasticity at single synapses. Neuropharmacology. 1998; 37:489–500. [PubMed: 9704990]

Markram H, Toledo-Rodriguez M, Wang Y, Gupta A, Silberberg G, Wu C. Interneurons of the neocortical inhibitory system. Nat Rev Neurosci. 2004; 5:793–807. [PubMed: 15378039]

Marsicano G, Lutz B. Expression of the cannabinoid receptor CB1 in distinct neuronal subpopulations in the adult mouse forebrain. Eur J Neurosci. 1999; 11:4213–4225. [PubMed: 10594647]

Marty S, Wehrle R, Sotelo C. Neuronal activity and brain-derived neurotrophic factor regulate the density of inhibitory synapses in organotypic slice cultures of postnatal hippocampus. J Neurosci. 2000; 20:8087–8095. [PubMed: 11050130]

McBain CJ, Fisahn A. Interneurons unbound. Nat Rev Neurosci. 2001; 2:11–23. [PubMed: 11253355]

McKinney RA, Debanne D, Gahwiler BH, Thompson SM. Lesion-induced axonal sprouting and hyperexcitability in the hippocampus in vitro: implications for the genesis of posttraumatic epilepsy. Nat Med. 1997; 3:990–996. [PubMed: 9288725]

Miles R, Toth K, Gulyas AI, Hajos N, Freund TF. Differences between somatic and dendritic inhibition in the hippocampus. Neuron. 1996; 16:815–823. [PubMed: 8607999]

Mitchell SJ, Silver RA. Shunting inhibition modulates neuronal gain during synaptic excitation. Neuron. 2003; 38:433–45. [PubMed: 12741990]

Morin F, Beaulieu C, Lacaille JC. Cell-specific alterations in synaptic properties of hippocampal CA1 interneurons after kainate treatment. J Neurophysiol. 1998; 80:2836–2847. [PubMed: 9862888]

Morishita W, Alger BE. Sr2+ supports depolarization-induced suppression of inhibition and provides new evidence for a presynaptic expression mechanism in rat hippocampal slices. J Physiol. 1997; 505(Pt 2):307–317. [PubMed: 9423174]

Oleskevich S, Clements J, Walmsley B. Release probability modulates short-term plasticity at a rat giant terminal. J Physiol. 2000; 524:513–523. [PubMed: 10766930]

Oleskevich S, Walmsley B. Synaptic transmission in the auditory brainstem of normal and congenitally deaf mice. J Physiol. 2002; 540:447–455. [PubMed: 11956335]

Pitkanen A, Immonen RJ, Grohn OH, Kharatishvili I. From traumatic brain injury to posttraumatic epilepsy: what animal models tell us about the process and treatment options. Epilepsia. 2009; 50(Suppl 2):21–29. [PubMed: 19187291]

Prince DA, Parada I, Scalise K, Graber K, Jin X, Shen F. Epilepsy following cortical injury: cellular and molecular mechanisms as targets for potential prophylaxis. Epilepsia. 2009; 50(Suppl 2):30–40. [PubMed: 19187292]

Prince DA, Tseng GF. Epileptogenesis in chronically injured cortex: in vitro studies. J Neurophysiol. 1993; 69:1276–1291. [PubMed: 8492163]

Rempe DA, Bertram EH, Williamson JM, Lothman EW. Interneurons in area CA1 stratum radiatum and stratum oriens remain functionally connected to excitatory synaptic input in chronically epileptic animals. J Neurophysiol. 1997; 78:1504–1515. [PubMed: 9310439]

Ribak CE, Bradburne RM, Harris AB. A preferential loss of GABAergic, symmetric synapses in epileptic foci: a quantitative ultrastructural analysis of monkey neocortex. J Neurosci. 1982; 2:1725–1735. [PubMed: 6815309]

Ribak CE, Harris AB, Vaughn JE, Roberts E. Inhibitory, GABAergic nerve terminals decrease at sites of focal epilepsy. Science. 1979; 205:211–214. [PubMed: 109922]

Ribak CE, Reiffenstein RJ. Selective inhibitory synapse loss in chronic cortical slabs: a morphological basis for epileptic susceptibility. Can J Physiol Pharmacol. 1982; 60:864–870. [PubMed: 7116231]

Roper SN, Eisenschenk S, King MA. Reduced density of parvalbumin- and calbindin D28-immunoreactive neurons in experimental cortical dysplasia. Epilepsy Res. 1999; 37:63–71. [PubMed: 10515176]

Rosen GD, Jacobs KM, Prince DA. Effects of neonatal freeze lesions on expression of parvalbumin in rat neocortex. Cereb Cortex. 1998; 8:753–761. [PubMed: 9863702]

Ross ST, Soltesz I. Selective depolarization of interneurons in the early posttraumatic dentate gyrus: involvement of the Na(+)/K(+)-ATPase. J Neurophysiol. 2000; 83:2916–2930. [PubMed: 10805688]

Sakaba T. Two Ca2+-dependent steps controlling synaptic vesicle fusion and replenishment at the cerebellar basket cell terminal. Neuron. 2008; 57:406–419. [PubMed: 18255033]

Salazar AM, Jabbari B, Vance SC, Grafman J, Amin D, Dillon JD. Epilepsy after penetrating head injury. I. Clinical correlates: a report of the Vietnam Head Injury Study. Neurology. 1985; 35:1406–1414. [PubMed: 3929158]

Scanziani M, Gahwiler BH, Charpak S. Target cell-specific modulation of transmitter release at terminals from a single axon. Proc Natl Acad Sci U S A. 1998; 95:12004–12009. [PubMed: 9751780]

Schwaller B, Tetko IV, Tandon P, Silveira DC, Vreugdenhil M, Henzi T, Potier MC, Celio MR, Villa AE. Parvalbumin deficiency affects network properties resulting in increased susceptibility to epileptic seizures. Mol Cell Neurosci. 2004; 25:650–663. [PubMed: 15080894]

Schwarzer C, Tsunashima K, Wanzenbock C, Fuchs K, Sieghart W, Sperk G. GABA(A) receptor subunits in the rat hippocampus II: altered distribution in kainic acid-induced temporal lobe epilepsy. Neuroscience. 1997; 80:1001–1017. [PubMed: 9284056]

Scotti AL, Bollag O, Kalt G, Nitsch C. Loss of perikaryal parvalbumin immunoreactivity from surviving GABAergic neurons in the CA1 field of epileptic gerbils. Hippocampus. 1997; 7:524–535. [PubMed: 9347349]

Shah MM, Anderson AE, Leung V, Lin X, Johnston D. Seizure-induced plasticity of h channels in entorhinal cortical layer III pyramidal neurons. Neuron. 2004; 44:495–508. [PubMed: 15504329]

Silva AV, Sanabria ER, Cavalheiro EA, Spreafico R. Alterations of the neocortical GABAergic system in the pilocarpine model of temporal lobe epilepsy: neuronal damage and immunocytochemical changes in chronic epileptic rats. Brain Res Bull. 2002; 58:417–421. [PubMed: 12183020]

Stewart BA, Mohtashami M, Trimble WS, Boulianne GL. SNARE proteins contribute to calcium cooperativity of synaptic transmission. Proc Natl Acad Sci U S A. 2000; 97:13955–13960. [PubMed: 11095753]

Sun QQ, Baraban SC, Prince DA, Huguenard JR. Target-specific neuropeptide Y-ergic synaptic inhibition and its network consequences within the mammalian thalamus. J Neurosci. 2003; 23:9639–9649. [PubMed: 14573544]

Sun QQ, Huguenard JR, Prince DA. Reorganization of barrel circuits leads to thalamically-evoked cortical epileptiform activity. Thalamus Relat Syst. 2005; 3:261–273. [PubMed: 18185849]

Tamas G, Buhl EH, Lorincz A, Somogyi P. Proximally targeted GABAergic synapses and gap junctions synchronize cortical interneurons. Nat Neurosci. 2000; 3:366–371. [PubMed: 10725926]

Tauck DL, Nadler JV. Evidence of functional mossy fiber sprouting in hippocampal formation of kainic acid-treated rats. J Neurosci. 1985; 5:1016–1022. [PubMed: 3981241]

Trotter SA, Kapur J, Anzivino MJ, Lee KS. GABAergic synaptic inhibition is reduced before seizure onset in a genetic model of cortical malformation. J Neurosci. 2006; 26:10756–10767. [PubMed: 17050714]

Tseng GF, Prince DA. Structural and functional alterations in rat corticospinal neurons after axotomy. J Neurophysiol. 1996; 75:248–267. [PubMed: 8822555]

Uematsu M, Hirai Y, Karube F, Ebihara S, Kato M, Abe K, Obata K, Yoshida S, Hirabayashi M, Yanagawa Y, et al. Quantitative chemical composition of cortical GABAergic neurons revealed in transgenic venus-expressing rats. Cereb Cortex. 2008; 18:315–330. [PubMed: 17517679]

Ulrich D, Huguenard JR. GABAB receptor-mediated responses in GABAergic projection neurones of rat nucleus reticularis thalami in vitro. J Physiol. 1996; 493(Pt 3):845–854. [PubMed: 8799904]

van den Pol AN, Obrietan K, Chen G. Excitatory actions of GABA after neuronal trauma. J Neurosci. 1996; 16:4283–4292. [PubMed: 8753889]

Vreugdenhil M, Jefferys JG, Celio MR, Schwaller B. Parvalbumin-deficiency facilitates repetitive IPSCs and gamma oscillations in the hippocampus. J Neurophysiol. 2003; 89:1414–1422. [PubMed: 12626620]

Wang Y, Gupta A, Toledo-Rodriguez M, Wu CZ, Markram H. Anatomical, physiological, molecular and circuit properties of nest basket cells in the developing somatosensory cortex. Cereb Cortex. 2002; 12:395–410. [PubMed: 11884355]

Weimer RM, Richmond JE, Davis WS, Hadwiger G, Nonet ML, Jorgensen EM. Defects in synaptic vesicle docking in unc-18 mutants. Nat Neurosci. 2003; 6:1023–1030. [PubMed: 12973353]

Wilcox KS, Dichter MA. Paired pulse depression in cultured hippocampal neurons is due to a presynaptic mechanism independent of GABAB autoreceptor activation. J Neurosci. 1994; 14:1775–1788. [PubMed: 8126570]

Williamson A, Patrylo PR, Spencer DD. Decrease in inhibition in dentate granule cells from patients with medial temporal lobe epilepsy. Ann Neurol. 1999; 45:92–99. [PubMed: 9894882]

Wittner L, Eross L, Czirjak S, Halasz P, Freund TF, Magloczky Z. Surviving CA1 pyramidal cells receive intact perisomatic inhibitory input in the human epileptic hippocampus. Brain. 2005; 128:138–152. [PubMed: 15548550]

Wittner L, Magloczky Z, Borhegyi Z, Halasz P, Toth S, Eross L, Szabo Z, Freund TF. Preservation of perisomatic inhibitory input of granule cells in the epileptic human dentate gyrus. Neuroscience. 2001; 108:587–600. [PubMed: 11738496]

Wyeth MS, Zhang N, Mody I, Houser CR. Selective reduction of cholecystokinin-positive basket cell innervation in a model of temporal lobe epilepsy. J Neurosci. 2010; 30:8993–9006. [PubMed: 20592220]

Xiang Z, Huguenard JR, Prince DA. Synaptic inhibition of pyramidal cells evoked by different interneuronal subtypes in layer v of rat visual cortex. J Neurophysiol. 2002; 88:740–750. [PubMed: 12163526]

Yamamoto K, Koyanagi Y, Koshikawa N, Kobayashi M. Postsynaptic cell type-dependent cholinergic regulation of GABAergic synaptic transmission in rat insular cortex. J Neurophysiol. 2010; 104:1933–1945. [PubMed: 20685921]

Zamecnik J, Krsek P, Druga R, Marusic P, Benes V, Tichy M, Komarek V. Densities of parvalbumin-immunoreactive neurons in non-malformed hippocampal sclerosis-temporal neocortex and in cortical dysplasias. Brain Res Bull. 2006; 68:474–481. [PubMed: 16459206]

Zhang N, Wei W, Mody I, Houser CR. Altered localization of GABA(A) receptor subunits on dentate granule cell dendrites influences tonic and phasic inhibition in a mouse model of epilepsy. J Neurosci. 2007; 27:7520–7531. [PubMed: 17626213]

Zhang W, Buckmaster PS. Dysfunction of the Dentate Basket Cell Circuit in a Rat Model of Temporal Lobe Epilepsy. J Neurosci. 2009; 29:7846–7856. [PubMed: 19535596]

Zhang W, Yamawaki R, Wen X, Uhl J, Diaz J, Prince DA, Buckmaster PS. Surviving Hilar Somatostatin Interneurons Enlarge, Sprout Axons, and Form New Synapses with Granule Cells in a Mouse Model of Temporal Lobe Epilepsy. J Neurosci. 2009; 29:14247–14256. [PubMed: 19906972]

Zucker RS, Regehr WG. Short-term synaptic plasticity. Annu Rev Physiol. 2002; 64:355–405. [PubMed: 11826273]

Bullet points

- Paired recordings in epileptogenic cortex were used to assess GABAergic inhibition
- Membrane properties of fast-spiking (FS) interneurons are normal in injured cortex
- Large decreases in GABA release from FS interneuronal terminals at their targets
- Multiple functional and structural abnormalities present in inhibitory terminals

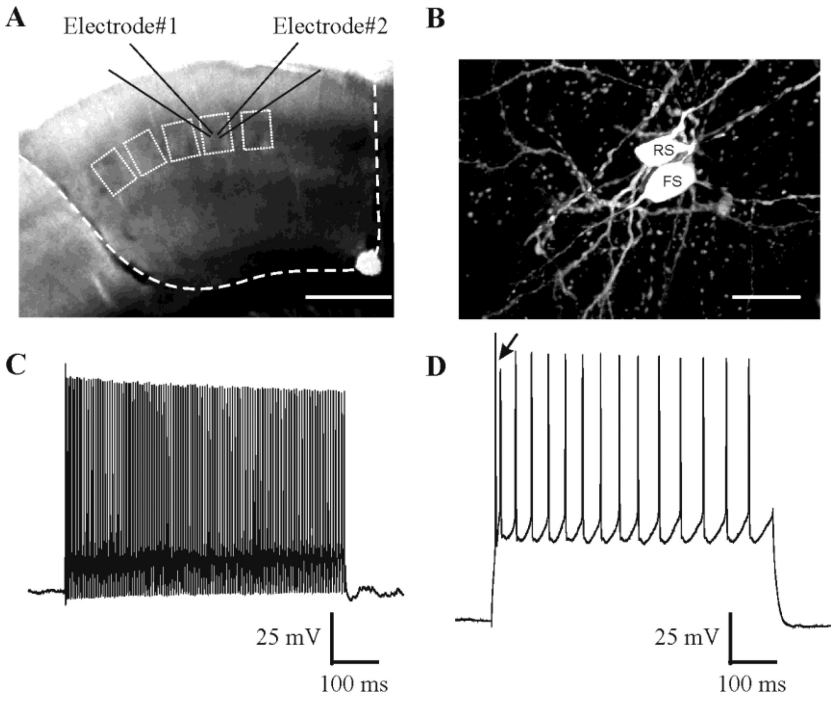

Fig. 1. Experimental schematic

A: Site of dual patch recording from a pair of neurons within a single barrel in unfixed in vitro coronal slice from somatosensory cortex. Dashed line: extent of undercutting and transcortical lesions. Small boxes: visualized barrels. Scale bar: 0.5 mm. B: Fluorescent image of a pair of cells filled with biocytin during a dual whole cell recording. FS: fast-spiking inhibitory interneuron; RS: excitatory regular-spiking neuron. Scale bar: 20 μm. C-D: Firing patterns of a FS cell (C; V_m -62 mV) and a RS cell (D; V_m -72 mV) evoked by 600 ms intracellular current pulses. Arrows in D indicate characteristic initial doublet-spiking in RS cells.

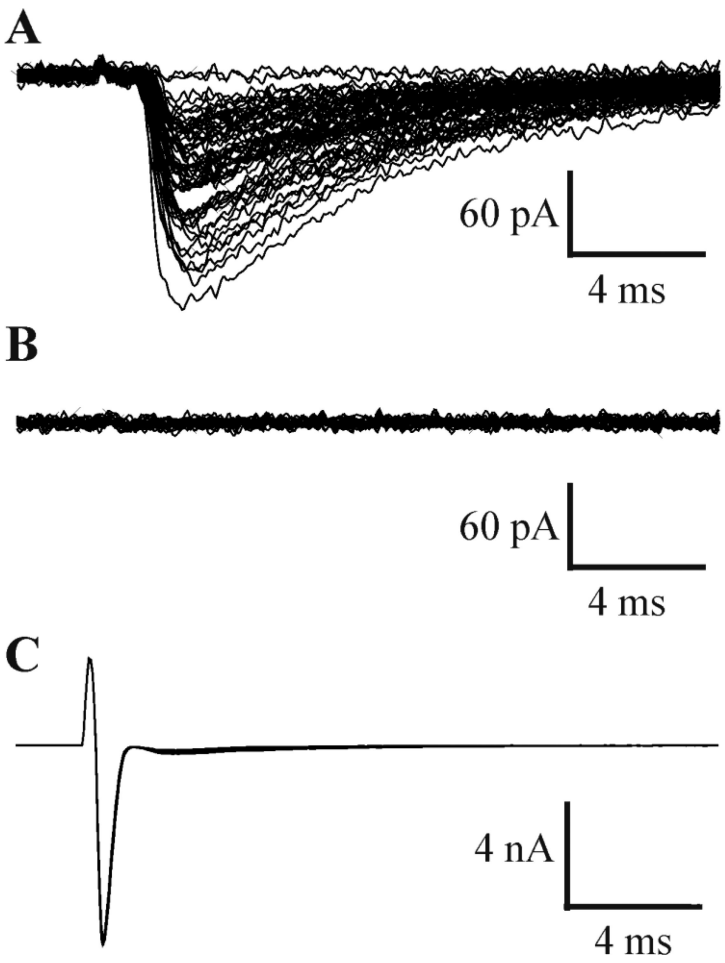

Fig. 2. Blockade of GABAergic responses by gabazine

A: Unitary inhibitory currents in a postsynaptic RS cell evoked by escape action currents in the presynaptic FS interneuron in C. B: Unitary IPSCs of A were completely blocked by adding drops of gabazine (10mM) directly to the bath. C: Presynaptic escape action currents in FS cells.

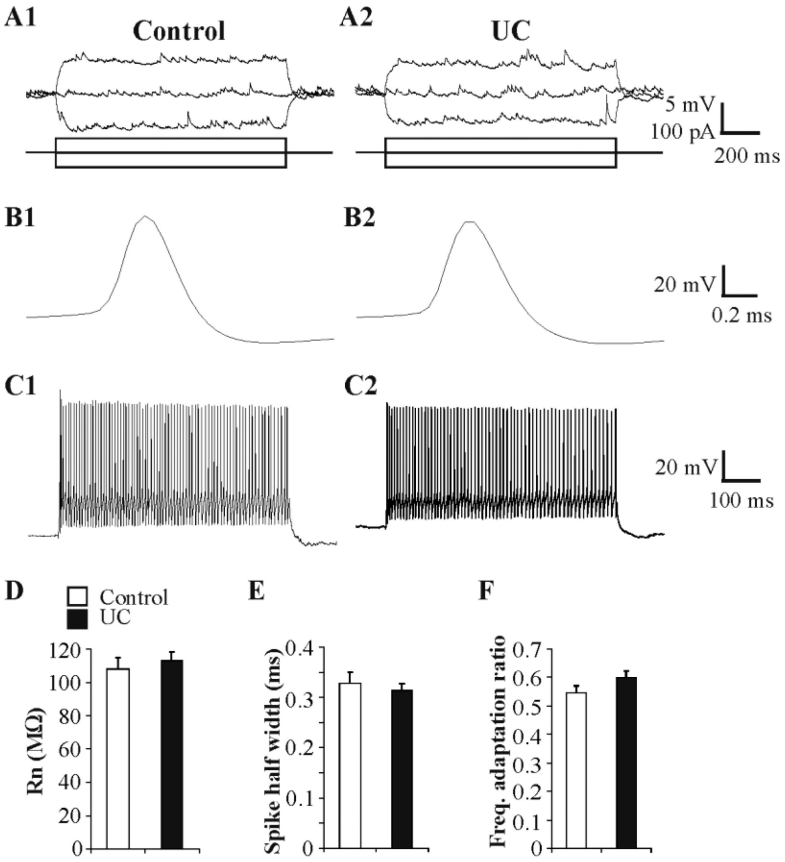

Fig. 3. Membrane properties of FS cells in control and UC slices

A: Representative current clamp responses of FS cells in control (A1) and UC groups (A2) to direct current injection (lower traces). B: Initial action potentials in trains from control (B1) and UC (B2) FS cells have similar spike half width. C: Spike trains (~110 Hz) evoked by 600 ms current pulses in representative control (C1, V_m -69 mV) and UC (C2, V_m -65 mV) FS cells. D-F: Bar graphs of input resistance (D; R_n), spike half width (E) and frequency adaptation ratio (ratio of the average frequency of last 5 APs to that of the initial 2 spikes in a 600ms train with firing frequency of ~110 Hz (F) in control (n = 29) and UC (n = 40) groups.

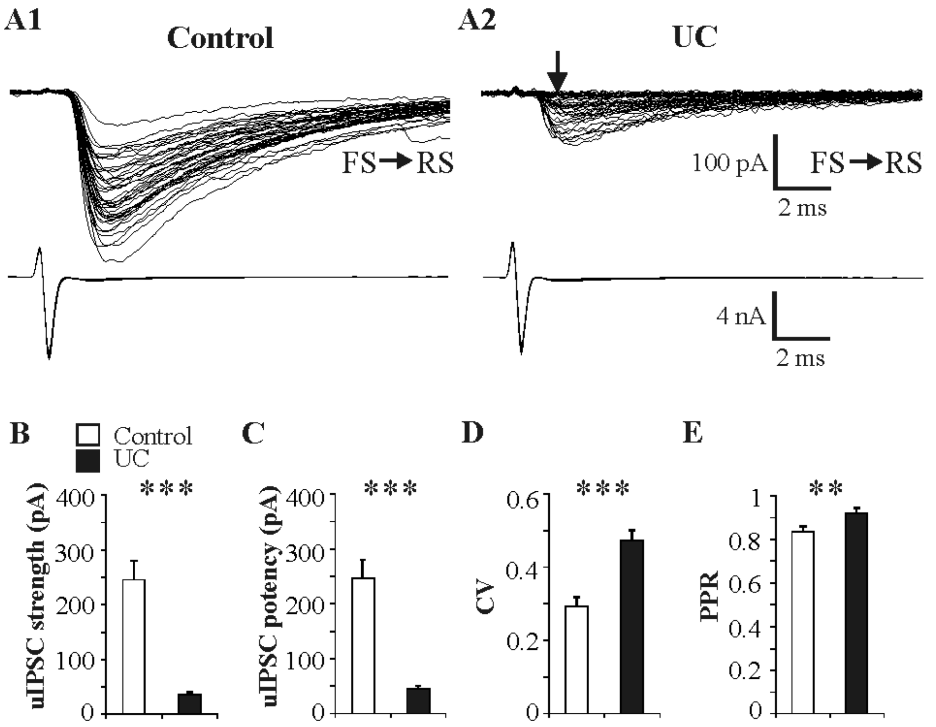

Fig. 4. Abnormalities of inhibitory synaptic transmission at FS-RS synapses in UC cortical slices

A: Representative superimposed traces from paired recordings of uIPSCs in a control RS (A1) and an UC RS cell (A2) evoked by single action currents in presynaptic FS neurons (lower traces). Unitary IPSCs in UC were smaller in amplitude and had increased failure rate (arrow in A2) vs. control. Twenty five/26 paired recordings in UC exhibited synaptic failures vs. 2/21 in control pairs. Scale bars in A2 for A1 and A2. B-E: Bar graphs show significantly decreased synaptic strength (B), reduced synaptic potency (C), increased coefficient of variation (CV) (D) and increased paired pulse ratio (PPR) (E) for uIPSCs in UC slices compared to control. Sample sizes are 21 pairs for all parameters in control and 26, 26, 26, 24 pairs in UC group for B-E, respectively. **: $P < 0.01$, ***: $P < 0.001$ in this and subsequent figures.

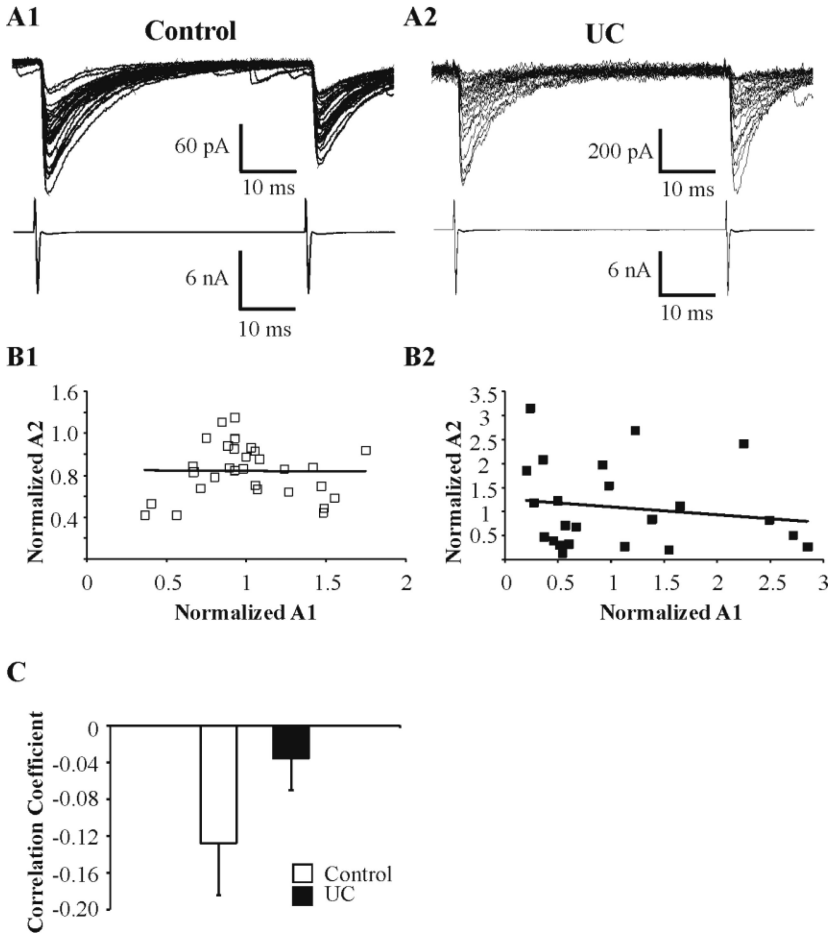

Fig. 5. Relationship of amplitudes of second and first uIPSCs evoked by paired stimuli at inter-pulse interval of 50 ms

A: Upper sweeps: Representative paired uIPSC responses in RS cells in control (A1) and UC (A2) slices. Lower traces: Presynaptic escape action currents in the FS cells of A1 and A2 pairs. B: Plots of normalized amplitudes of the 1st vs. 2nd uIPSCs shown in panel A. Each symbol represents one pair of uIPSCs. Solid lines indicate the linear regression lines (correlation coefficient: 0.008 in B1, -0.162 in B2). C: Bar graph of correlation coefficient for pairs from control (-0.13, n = 21) and UC (-0.04, n = 24). *: $P < 0.05$.

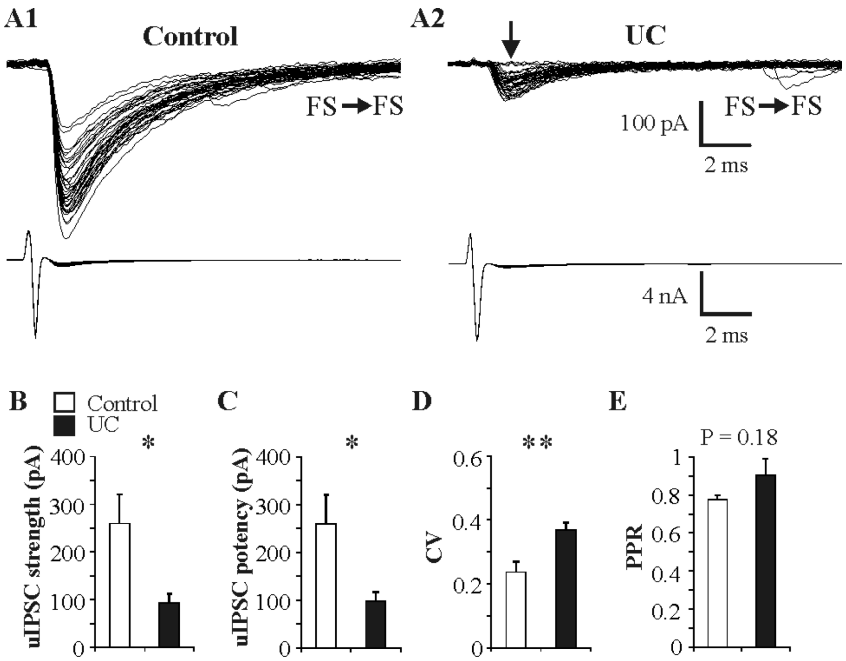

Fig. 6. Abnormalities of inhibitory transmission at FS-FS synapses

A1-A2: Representative superimposed uIPSCs (upper traces) in control (A1) and UC (A2) FS cells evoked at 0.33 Hz by action currents in presynaptic FS cells (lower traces). Arrow in A2: synaptic failures were found in 5/10 UC pairs and 0/7 controls. Decreased uIPSC amplitude present in A2. B-E: Analysis of uIPSC properties in 7 control and 10 UC pairs shows decreased synaptic strength (B), reduced synaptic potency (C) and increased CV (D) with no significant difference in PPR (E) in UC vs. control slices.

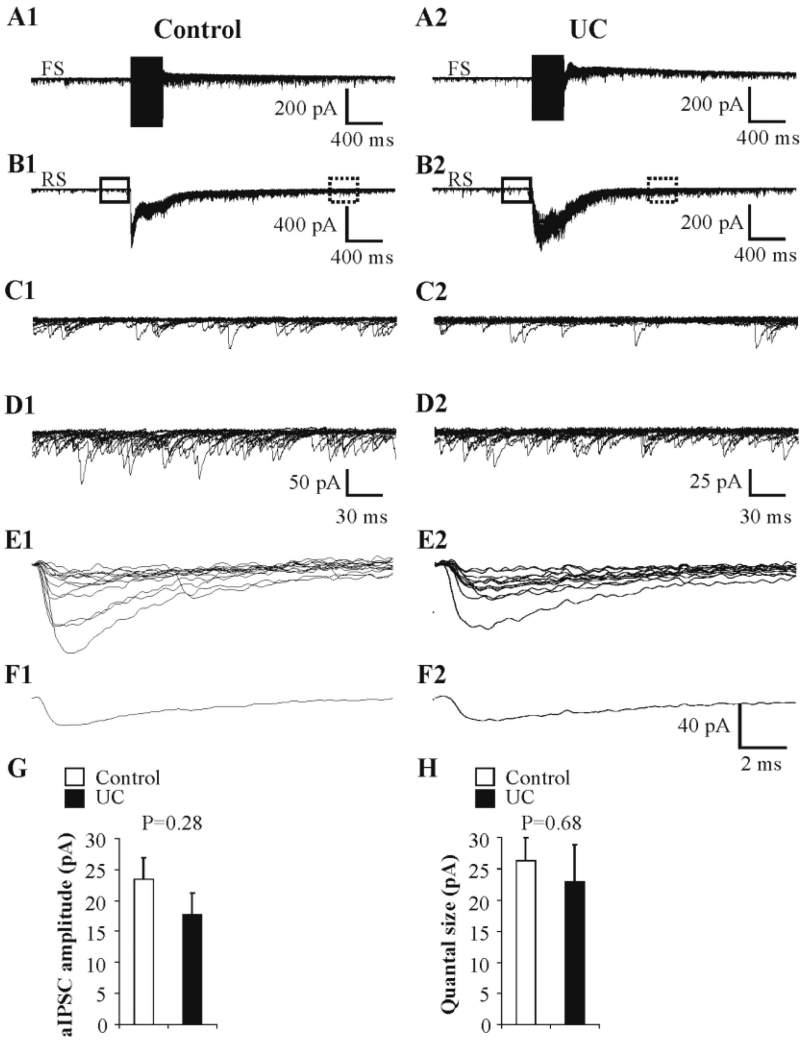

Fig. 7. Quantal size at FS-to-RS synapses

A, B: High frequency action current trains in FS cell (A; 250 Hz, 350 ms) evoked barrage of uIPSCs in postsynaptic RS cell (B), followed by robust asynchronous IPSCs (aIPSCs), presumably due to quantal release at autaptic (A) and FS-RS (B) synapses in both control (A1, B1) and UC (A2, B2) slices. Fifteen sweeps superimposed. C1, C2: Spontaneous IPSCs in postsynaptic RS cells from segments within solid boxes prior to stimulus trains in B1, B2, respectively, displayed at increased gain and faster time base. D1, D2: Higher frequency of aIPSCs from segments of traces within dashed boxes of B1 and B2, respectively, shown at higher gain and faster time base. E1,E2: Representative quantal IPSCs evoked in low Ca^{2+} / high Mg^{2+} ACSF obtained in control (E1; n = 13 events) and UC (E2; n = 12 events) pairs (Methods). F1,F2: Average traces of corresponding quantal responses in E1, E2, respectively. G: Bar graph of average amplitudes of aIPSCs in postsynaptic RS cells in control (n = 5) and UC (n = 5) paired recordings. H: Bar graph of average amplitudes of quantal events evoked at control (n = 5) and UC (n = 4) synapses.

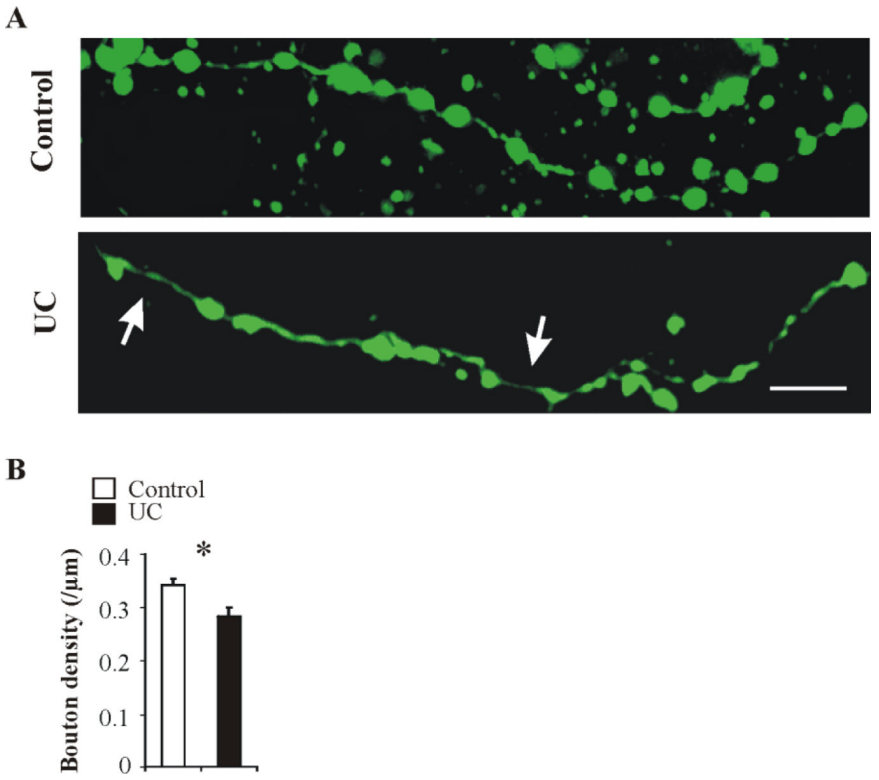

Fig. 8. Reduced bouton density in UC FS cells

A: Representative confocal images of biocytin (green) immunoreactivity in axonal segments from a control (upper panel) and a UC (lower panel) FS cell. Arrows in lower panel point to gaps without boutons along the axon. Calibration: 10 μm. B: UC FS cells (n = 4) had lower axonal bouton density compared to controls (n = 4). *: $P < 0.05$.

TABLE 1

Synaptic kinetics and latency of uIPSCs in naive and undercut cortex

Connection	90-10% decay time		10-90% rise time		Latency	
	Control	Undercut	Control	Undercut	Control	Undercut
FS - RS	16.4 ± 0.8 (21)	15.2 ± 0.8 (23)	0.66 ± 0.02 (21)	0.67 ± 0.03 (23)	0.85 ± 0.04 (21)	0.82 ± 0.03 (26)
FS - FS	9.3 ± 1.9 (7)	8.3 ± 0.7 (10)	0.51 ± 0.04 (7)	0.47 ± 0.01 (8)	0.72 ± 0.08 (7)	0.72 ± 0.04 (10)

All data are represented as mean ± SEM. Sample sizes are included in parentheses. Data unit is ms for all numbers. FS: inhibitory fast-spiking cells, RS: excitatory regular-spiking cells.